British Journal of Pharmacology

DOI:10.1111/j.1476-5381.2011.01545.x
www.brjpharmacol.org

RESEARCH PAPER

Indolinones and anilinophthalazines differentially target VEGF-A- and basic fibroblast growth factor-mediated responses in primary human endothelial cells

AM Latham[1], AF Bruns[1], J Kankanala[2], AP Johnson[2], CWG Fishwick[2], S Homer-Vanniasinkam[3] and S Ponnambalam[1]

[1]*Endothelial Cell Biology Unit, Institute of Molecular and Cellular Biology, University of Leeds, Leeds, UK,* [2]*School of Chemistry, University of Leeds, Leeds, UK, and* [3]*Leeds Vascular Institute, Leeds General Infirmary, Leeds, UK*

Correspondence
S. Ponnambalam, Endothelial Cell Biology Unit, Institute of Molecular and Cellular Biology, University of Leeds, Leeds LS2 9JT, UK. E-mail: s.ponnambalam@leeds.ac.uk

Keywords
VEGFR2; FGFR1; kinase inhibitor; endothelium; angiogenesis

Received
5 January 2011
Revised
13 May 2011
Accepted
6 June 2011

BACKGROUND AND PURPOSE

The potent pro-angiogenic growth factors VEGF-A and basic fibroblast growth factor (bFGF) exert their effects by binding VEGF receptor 2 and FGF receptor tyrosine kinases, respectively. Indolinones (e.g. SU5416 and Sutent) and anilinophthalazines (e.g. PTK787) are potent small molecule inhibitors of VEGFR2 and other tyrosine kinases, but their effects on VEGF-A- and bFGF-stimulated endothelial responses are unclear. Here we assess the ability of these compounds to inhibit pro-angiogenic responses through perturbation of receptor activity and endothelial function(s).

EXPERIMENTAL APPROACH

We used *in silico* modelling, *in vitro* tyrosine kinase assays, biochemistry and microscopy to evaluate the effects of small molecules on receptor tyrosine kinase activation and intracellular signalling. Primary human endothelial cells were used to assess intracellular signalling, cell migration, proliferation and tubulogenesis.

KEY RESULTS

We predicted that the anilinophthalazine PTK787 binds the tyrosine kinase activation loop whereas indolinones are predicted to bind within the hinge region of the split kinase domain. Sutent is a potent inhibitor of both VEGFR2 and FGFR1 tyrosine kinase activity *in vitro*. The compounds inhibit both ligand-dependent and -independent VEGFR2 trafficking events, are not selective for endothelial cell responses and inhibit both VEGF-A- and bFGF-mediated migration, wound healing and tubulogenesis at low concentrations.

CONCLUSIONS AND IMPLICATIONS

We propose that these compounds have novel properties including inhibition of bFGF-mediated endothelial responses and perturbation of VEGFR2 trafficking. Differential inhibitor binding to receptor tyrosine kinases translates into more potent inhibition of bFGF- and VEGF-A-mediated intracellular signalling, cell migration and tubulogenesis. Indolinones and anilinophthalazines thus belong to a class of multi-kinase inhibitors that show clinical efficacy in disease therapy.

Abbreviations

bFGF, basic fibroblast growth factor; FGFR1, fibroblast growth factor receptor 1; HUVECs, human umbilical vein endothelial cells; pHFF, primary human foreskin fibroblasts; PTK787 (vatalanib), N-(4-chlorophenyl)-4-(pyridin-4-ylmethyl)phthalazin-1-amine; VEGFR2, VEGF receptor 2; SU5416 (semaxanib), (3Z)-3-[(3,5-dimethyl-1H-pyrrol-2-yl)methylidene]-1,3-dihydro-2H-indol-2-one

Introduction

The growth, invasion and metastasis of a tumour are heavily dependent on the sprouting of new blood vessels, that is, angiogenesis. This neovascularization is dependent on transformed cells secreting a cocktail of soluble pro-angiogenic proteins including VEGFs and fibroblast growth factors (FGFs). These proteins can stimulate endothelial cell migration, proliferation and the formation of capillary tubes, all key steps in angiogenesis (Carmeliet, 2003). The VEGF gene family encodes soluble secreted cytokines such as VEGF-A, VEGF-B, VEGF-C, VEGF-D and placental growth factor (Ferrara *et al*., 2003; Latham *et al*. 2010). These ligands bind membrane VEGF receptor tyrosine kinases (VEGFR1–3) where VEGFR2 is a key mediator of VEGF-A-stimulated pro-angiogenic intracellular signalling (Olsson *et al*. 2006; Holmes *et al*., 2007). In comparison, FGFs are a diverse family of potent mitogens, which bind specific FGF receptor tyrosine kinases (FGFR1–4), of which the FGFR1iiic isoform is the most highly expressed in endothelial cells (Murakami *et al*. 2008; Oguro *et al*., 2010). De-regulated FGFR signalling has been implicated in breast cancer, prostate cancer and multiple myeloma (Knights and Cook, 2010). VEGFR and FGFR are members of the Type III receptor tyrosine kinase subfamily comprising a large extracellular domain, a single transmembrane region and a cytoplasmic split tyrosine kinase domain (Holmes *et al*., 2007). Growth factor binding to cognate receptors promotes receptor dimerization, tyrosine kinase activation and *trans*-autophosphorylation of specific tyrosine residues within the cytoplasmic domain (Holmes *et al*., 2007). Various SH2 domain-containing proteins are recruited to phosphotyrosine residues, including phosphoinositide-specific phospholipase Cγ1 (PLCγ1) (Takahashi and Shibuya, 1997). VEGFR2 and FGFR signalling pathways share common events including activation of c-Akt (PKB) and ERK1/2 (p42/44 MAPK) (Takahashi and Shibuya, 1997; Blanes *et al*. 2007; Knights and Cook, 2010). Upon ligand stimulation, VEGFR2 undergoes a co-ordinated programme of trafficking and proteolysis linked to PKC activation, ubiquitination and proteasomal degradation (Bruns *et al*., 2010). The VEGFR2 gene is essential, as knockout mice display embryonic lethality with almost complete loss of endothelial cells and defective vasculogenesis (Shalaby *et al*., 1995). Constitutive activation of FGFR1 in mice can induce mammary invasive lesions and prostate cancer (Turner and Grose, 2010).

There is much interest in the development of membrane permeable molecules that target receptor tyrosine kinases such as VEGFR2 and FGFR and thereby block tumour angiogenesis (Jain, 2007). Indolinones are one such class of ATP-style mimetics that bind the VEGFR2 tyrosine kinase domain and inhibit enzyme activity, exemplified by the anti-cancer drug SU11248 (sunitinib or Sutent) and its predecessor compound SU5416 (Noble *et al*., 2004). These compounds are characterized by a 2-oxindole core with a variant side chain at the 3-position. Sutent has been approved for treatment of renal cell carcinoma and imatinib-resistant gastrointestinal stromal tumours (Roskoski, 2007). Another class of tyrosine kinase inhibitors are anilinophthalazines such as PTK787 (vatalanib or ZK 222548). These compounds contain a phthalazine or quinazoline heterocycle with multiple substitutions. PTK787 has been shown to inhibit development of the microvasculature and multiple myeloma growth (Lin *et al*., 2002) and has shown promise for the treatment of advanced metastatic colorectal cancer (Los *et al*., 2007).

The mechanism of action of these compounds on VEGFR2 has been well characterized *in vitro*; however, the specificity of indolinones and anilinophthalazines is unclear as they have been shown to inhibit a variety of Type III receptor tyrosine kinases (Wood *et al*., 2000; Jubb *et al*., 2006; Chow and Eckhardt, 2007). It is becoming increasingly clear that inhibition of multiple pro-angiogenic axes may offer a better therapy than targeting only one pathway or a single enzymatic step (Knights and Cook, 2010; Oguro *et al*. 2010). In this study, we have examined the ability of these compounds to target either the VEGF-A-VEGFR2 or bFGF-FGFR axes, with consequences for endothelial cell migration, wound healing and tube formation, all key features of angiogenesis.

Methods

Reagents

Human umbilical vein endothelial cells (HUVECs) were retrieved from human tissues obtained by local ethical approval from the Leeds Hospitals NHS Trust and cultured as previously described (Howell *et al*., 2004). Recombinant human VEGF-A was a gift from Genentech (San Francisco, CA, USA). Recombinant human EGF, bFGF, VEGFR2 and FGFR1iiic and antibodies against VEGFR1 and VEGFR2 extracellular domain were purchased from R&D Systems (Minneapolis, MN, USA). Phospho-ERK1/2, phospho-PLCγ1 and ERK1/2 antibodies were purchased from Cell Signalling Technology (Danvers, MA, USA). FGFR1, PLCγ1 and PECAM-1 antibodies were from Santa Cruz Biotechnology (CA, USA). Antibody to early endosomal antigen-1 (EEA-1) was from BD Biosciences and horseradish peroxidase (HRP)-conjugated secondary antibodies were from PerBio Sciences (Cramlington, UK). AlexaFluor-conjugated secondary antibodies and Concanavalin A were from Invitrogen (Amsterdam, the Netherlands). SU5416 (Calbiochem), Sutent (Alexis Biochemicals) and PTK787 (Novartis Pharma Inc.) were prepared as 10 mM stock solutions in dimethyl sulphoxide (DMSO). Serial 10-fold dilutions were made in tissue culture medium. Unless otherwise stated, inhibitors were used at 1 μM (SU5416) and 100 nM (Sutent or PTK787). These were deemed to be submaximal concentrations displaying ~90% VEGFR2 inhibition. All other reagents were obtained from Sigma-Aldrich (Poole, UK) unless otherwise stated.

In silico *modelling*

SU5416, Sutent and PTK787 were docked into the crystal structures of VEGFR2 (3cjg and 3efl) (Harris *et al*., 2008; Tasker and Patel, 2008) and FGFR1 (3ky2) (Bae *et al*., 2010) using the Glide programme (Schrödinger LLC, 2004) (Friesner *et al*., 2004) and hydrogen bond contacts established. The binding mode of PTK787 was validated against a related anilinophthalazine, motesanib. Log dissociation constants (pKi) of the competitive inhibitors for the receptors were predicted using the SPROUT programme (SPROUT Software Package, SimBioSys Inc., 2005) (Ali *et al*., 2005).

^{33}P receptor tyrosine kinase HotSpot^{SM} profiling assay

Full-length recombinant VEGFR2 or FGFR1 was incubated with 25 μM (radiolabelled) [γ^{33}P]-ATP and $MgCl_2$ together with threefold serial dilutions of inhibitors starting at 10, 50 and 100 μM. Inhibition of kinase activity was assessed by measuring the relative reduction of the γ^{33}P signal produced by autophosphorylation events on recombinant receptor (Reaction Biology, Malvern, PA, USA).

Immunoblotting

HUVECs were deprived of serum in MCDB-131 (Invitrogen) supplemented with 0.2% (w/v) BSA for 3 h and pretreated with inhibitors for 1 h before stimulation with 25 ng·mL^{-1} VEGF-A or bFGF for 7.5 min in the presence of inhibitors. Cells were then lysed in 2% (w/v) SDS in PBS and lysates scraped into centrifuge tubes. Lysates were boiled and sonicated briefly before protein content was quantified using the bicinchoninic acid assay. Samples were resuspended in SDS-PAGE sample buffer and boiled for 5 min prior to electrophoresis. Proteins were transferred to nitrocellulose membranes and probed with appropriate antibodies. Immunoreactive proteins were visualized by enhanced chemiluminescence using a Fuji LAS-3000 imaging system (Raytek Scientific, Sheffield, UK). Band intensity was quantified by two-dimensional densitometry using *AIDA* software (Fujifilm, Fuji, Japan).

Cell surface biotinylation

HUVECs in six-well plates were treated as appropriate, washed in PBS and incubated with 0.5 mg·mL^{-1} biotin (Thermo Scientific, IL) in PBS containing 2 mM $MgCl_2$; 2 mM $CaCl_2$ for 45 min on ice with gentle agitation. Biotinylation was quenched in Tris-buffered saline and cells lysed for 1 h on ice in radioimmunoprecipitation (RIPAE) buffer [1% (v/v) Nonidet P-40; 0.5% (w/v) sodium deoxycholate; 0.1% (w/v) SDS; 5 mM EDTA; 1 mM Na_3VO_4; 1 mM NaF; Sigma protease inhibitor cocktail in PBS]. Lysates were centrifuged at 16 000× *g* for 30 min at 4°C and supernatant containing equal amounts of protein incubated with neutravidin-agarose beads (Thermo Scientific) for 16 h at 4°C with gentle agitation. Beads were washed three times in lysis buffer, proteins eluted in SDS-PAGE sample buffer and subjected to electrophoresis and immunoblotting.

Immunofluorescence microscopy

Immunofluorescence microscopy was performed as previously described (Ewan *et al.*, 2006). Cells were deprived of serum for 3 h and pretreated with chemical inhibitors for 1 h prior to stimulation with 25 ng·mL^{-1} VEGF-A or bFGF for 1 h in the presence of inhibitors. Cells were fixed in formalin, permeabilized and stained with appropriate antibodies and DAPI. Slides were analysed using a wide-field deconvolution microscopy system (Howell *et al.*, 2004).

Flow cytometry

Cells were deprived of serum, pretreated with inhibitors and stimulated with VEGF-A as described above. Live cells were then removed from the culture dish using Type II collagenase; 5 mM EDTA and the cell surface stained with anti-VEGFR2 followed by Cy5-conjugated secondary antibody (Jackson Immunoresearch Labs, PA) and fixed in 1% (w/v) paraformaldehyde. Cell surface levels of VEGFR2 were analysed using flow cytometry by counting 10 000 events per condition (BD FACSCalibur™).

Scratch wound healing assay

Confluent HUVECs were deprived of serum for 3 h and pretreated with chemical inhibitors for 1 h before a vertical scratch wound was made through the cell monolayer with a 1 mL plastic pipette with 0.9 mm tip width. Scratched cell monolayers were washed with PBS, photographed and stimulated with 25 ng·mL^{-1} VEGF-A or bFGF during a 24 h recovery period and analysis of wound closure was monitored using digital microscopy. HeLa and primary human foreskin fibroblast (pHFF) cells were cultured in Dulbecco's modified Eagle medium (DMEM) (Invitrogen) during wound healing assays. Wound closure was calculated using NIH Image J software and represented as % after calculating [(width before – width after)/width before] × 100.

Bromodeoxyuracil (BrdU) cell proliferation assay

HUVECs were seeded at 2000 cells per well in 96-well plates, treated with inhibitors for 16 h and incubated with 10 μM BrdU for 2 h. A cell proliferation ELISA (Roche Diagnostics) was carried out according to manufacturer's instructions. ELISAs were developed using 3,3′,5,5′-tetramethylbenzidine solution and reaction stopped with 1 M H_2SO_4. Absorbance at 450 nm was measured.

Cell viability assay

Cell viability was measured using the 3-(4,5-dimethylthiazol-2-yl)-5-(3-carboxymethoxyphenyl)-2-(4-sulfophenyl)-2H-tetrazolium (MTS) assay. HUVECs were seeded at 2000 cells per well in 96-well plates, treated with inhibitors for 16 h and incubated with 20 μL CellTiter 96® AQueous One Solution Reagent (Promega) for 4 h until sufficient colour change had been reached. Absorbance at 490 nm was measured.

Transwell cell migration assay

Confluent HUVECs were trypsinized and seeded at 60 000 cells per well into a 24-well plate with 8 μm pore size Transwell inserts (Corning, NY) containing inhibitor in both the upper and lower chamber and 50 ng·mL^{-1} VEGF-A, bFGF or EGF in the lower chamber for migration to occur. After 16 h, filters were fixed, stained with haematoxylin-eosin and excised for microscopy. Random fields from each image were counted for calculation of % number of cells migrated onto filter underside.

Fibroblast co-culture assay

pHFFs were grown to confluence in a 48-well plate in DMEM and then 7500 HUVECs seeded as a secondary layer in a two-cell co-culture model. After 24 h the co-culture was incubated in endothelial growth medium supplemented with 25 ng·mL^{-1} VEGF-A or bFGF and either DMSO or appropriate drug for 7 days. The co-cultures were fixed and stained for the endothelial specific marker PECAM-1 and further with anti-

Table 1

Comparison of estimated binding affinities (pKi values) of indolinones and anilinophthalazines to VEGFR2 and FGFR1 kinases *in silico*, as predicted using SPROUT programme (see *Methods*)

Inhibitor	Estimated pKi VEGFR2	FGFR1
SU5416	–7.40	–7.08
Sutent	–9.21	–8.05
PTK787	–10.49	–8.30

mouse HRP. Tubes were visualized under a light microscope using cobalt-enhanced 1,1,diaminobenzidine/urea/hydrogen peroxide development.

Results

Indolinones and anilinophthalazines are predicted to bind in the ATP binding pocket of VEGFR2 and FGFR1 with high affinity

Membrane-permeable, ATP-competitive compounds (ATP analogues) can bind protein kinase domains and inhibit enzyme activity (Zhang *et al.*, 2009). To test the rationale that indolinones and anilinophthalazines bind both VEGFR2 and FGFR1 we used an *in silico* modelling approach to predict both the binding mode and affinity of the compounds to the respective tyrosine kinase domains. All three inhibitors were predicted to bind VEGFR2 and FGFR1 with a pKi of –7 or less (corresponding to predicted binding affinities in the nanomolar range, Table 1). SU5416 was predicted to exhibit the weakest binding affinity to both receptors, whereas PTK787 was predicted to have the strongest. All three inhibitors were predicted to bind VEGFR2 with greater affinity than FGFR1 (Table 1). The indolinones (SU5416 and Sutent) are predicted to make hydrogen bond contacts with Glu^{915} and Cys^{919} in the hinge region of the ATP-binding pocket of VEGFR2. Similarly, they are predicted to make contacts with the equivalent residues in FGFR1, Glu^{562} and Ala^{564} (Figure 1). However, anilinophthalazines are predicted to display a different binding mode. While PTK787 makes contact with Cys^{919} of VEGFR2, it also binds Asp^{1046} in the activation loop Asp-Phe-Gly (DFG) residue motif. PTK787 also makes contact with Asp^{641} in the DFG motif of FGFR1 (Figure 1). The difference in predicted binding affinity for the two receptors is greatest for PTK787 with tighter binding predicted to VEGFR2 (Table 1).

Indolinones and anilinophthalazines differentially inhibit VEGFR2 and FGFR1 tyrosine kinase activity in vitro *and VEGF-A- and bFGF-mediated signalling in endothelial cells*

To test the effects of indolinones and anilinophthalazines on the intrinsic tyrosine kinase activity of VEGFR2 and FGFR1 we used an *in vitro* kinase assay. SU5416, Sutent and PTK787 all showed dose-dependent inhibition of purified recombinant VEGFR2 and FGFR1 tyrosine kinase activity, although SU5416 exhibited only ~55% inhibition of kinase activity at a high concentration of 10 μM (Figure 2). Sutent and PTK787 showed similar inhibitory profiles for VEGFR2 (IC_{50} ~ 0.3–0.6 μM). Both drugs began to inhibit VEGFR2 kinase activity at a concentration of ~10 nM and a concentration of 10 μM elicited ~90% inhibition of VEGFR2 kinase activity *in vitro* (Figure 2A). In keeping with our prediction derived from modelling, Sutent displayed similarly potent inhibition of FGFR1 but PTK787 is a much weaker inhibitor of this receptor, indicating greater selectivity towards VEGFR2 (Table 2). The indolinone SU5416 is the least potent inhibitor of VEGFR2 (IC_{50} ~9 μM; Figure 2A) and displayed similar inhibition of FGFR1 (IC_{50} ~ 14 μM; Figure 2B).

The VEGFR2 and FGFR-regulated intracellular signalling pathways involve phosphorylation of serine, threonine and tyrosine residues on effector proteins. These include the generation of PLCγ1-pY783, c-Akt-pS473 and the dual phosphorylated ERK1/2-pT202/pY204. Phosphorylation of these proteins activates enzymatic activity and influences endothelial cell migration, proliferation and survival (Olsson *et al.*, 2006). The effects of SU5416, Sutent and PTK787 on VEGF-A- and bFGF-mediated downstream signalling were examined by immunoblotting in primary endothelial cells. All three compounds dose-dependently inhibited VEGFR2 Y1175 phosphorylation, a key hallmark of VEGFR2 activation that stimulates pro-angiogenic responses by endothelial cells (Figure 3). One question is the nature of the cellular target of bFGF in endothelial cells. To test a role for FGFR1, we immunoprecipitated all tyrosine phosphorylated proteins from bFGF-stimulated cells and immunoblotted for FGFR1 (Figure S1). Surprisingly, we could not detect FGFR1 phosphorylation in bFGF-stimulated cells (Figure S1), suggesting that the effects of this growth factor could be mediated through another FGFR or FGFR-like receptor. However, all three compounds showed dose-dependent inhibition of both VEGF-A- and bFGF-stimulated PLCγ1 and ERK1/2 phosphorylation (Figures 3 and S2). Inhibition of VEGF-A-mediated signalling by SU5416 displays a very steep IC_{50} curve: immunoblots show that inhibition of VEGFR2, PLCγ1 and ERK1/2 phosphorylation are pronounced at 100 nM, but the compound shows little inhibitory effect below this concentration, giving the inhibition an 'all-or-nothing' profile at the chosen drug concentrations (Figure 3A). Sutent and PTK787 are more potent inhibitors of VEGF-A-mediated signalling but displayed shallower IC_{50} profiles (Figure 3B and C). Sutent inhibits its bFGF-mediated signalling at 100 nM (Figure 3B). In contrast PTK787 and SU5416 are less potent; however, they still completely abolished bFGF-stimulated PLCγ1 and ERK1/2 phosphorylation at 5 μM and 10 μM, respectively (Figure 3A and C).

Inhibition of VEGFR2 tyrosine kinase activity alters receptor trafficking and degradation

VEGFR2 undergoes clathrin-mediated endocytosis and is recycled between the cell surface and endosomes (Ewan *et al.*, 2006). Activated VEGFR2 co-distributes with the ESCRT-0 complex (Hrs/STAM) on early endosomes before trafficking through late endosomes in a pathway linked to lysosomal

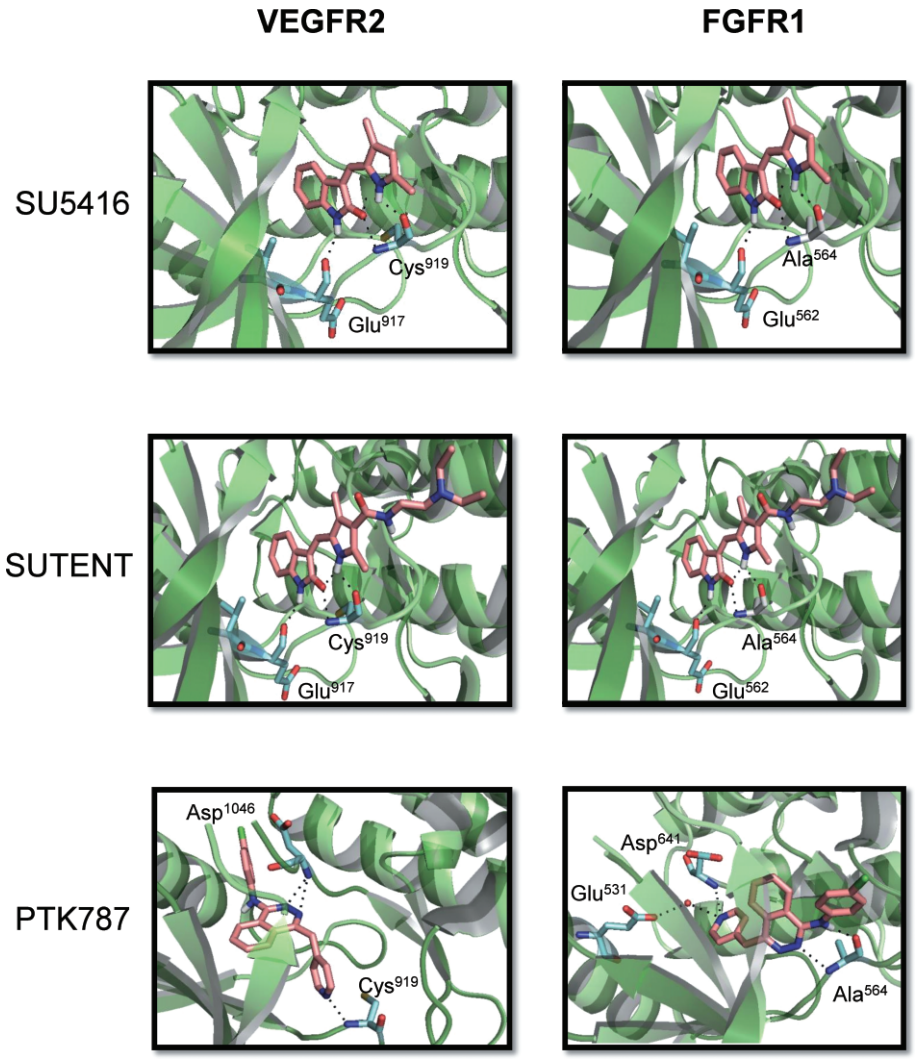

Figure 1

Prediction of binding by indolinones and anilinophthalazines to VEGFR2 and FGFR1 tyrosine kinase domains. SU5416, Sutent and PTK787 were docked into VEGFR2 and FGFR1 tyrosine kinase domains using the Glide programme to predict binding pose and hydrogen bond contacts formed (see Methods). Pink carbon backbones denote inhibitors; turquoise carbon backbones denote key amino acid residues in tyrosine kinase domain; black dotted lines denote hydrogen bonds; lone red circle denotes water molecule.

degradation (Ewan *et al.*, 2006). How is VEGFR2 trafficking affected by inhibition of tyrosine kinase activity? Under steady-state conditions, VEGFR2 localized to the plasma membrane, endosomes and a biosynthetic pool associated with the Golgi apparatus (Figures S3A, 4A and B). VEGF-A stimulation for 60 min caused significant VEGFR2 internalization and partial co-distribution with the EEA-1 endosomal marker protein (Figure 4A). In non-permeabilized cells, plasma membrane staining of VEGFR2 was decreased after VEGF-A stimulation (Figure 4B). In the presence of both SU5416 and VEGF-A for 60 min, VEGFR2 was arrested at the plasma membrane (Figure 4B). We have previously shown that upon blocking new protein synthesis, SU5416 caused retention of VEGFR2 within late endosomes after prolonged VEGF-A stimulation (Ewan *et al.*, 2006). In the studies shown here, we also detected a significant VEGFR2 pool remaining at the plasma membrane after ligand stimulation for shorter time points. VEGF-A stimulation for 60 min in the presence of Sutent or PTK787 (Figure 4A and B) caused similar levels of VEGFR2 accumulation at the plasma membrane as with SU5416. Note that VEGFR2 staining in HUVECs shows an inherently heterogeneous pattern; representative cells are shown (Figure 4A and B). The effects of the inhibitors were confirmed using cell surface biotinylation studies (Figure 4C) and quantified using flow cytometry to assess VEGFR2 levels on the surface of endothelial cells (Figure 4D). Immunoblotting of cell lysates and biotinylated cell surface proteins revealed that indolinones and anilinophthalazines inhibit both VEGF-A-stimulated internalization and degradation of VEGFR2 in HUVECs. However, at the concentrations used in this study, SU5416 and Sutent each had a slightly greater inhibitory effect than PTK787 (Figure 4C). Using flow cytometry, a ~35% decrease in cell surface VEGFR2 levels was observed after VEGF-A stimulation for 60 min (Figure 4D).

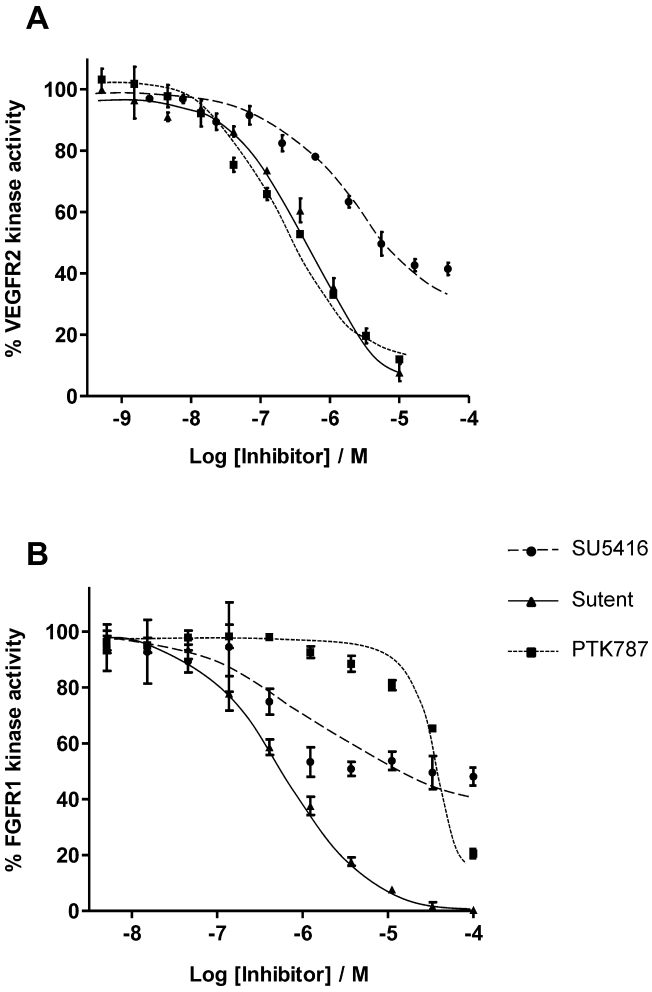

Figure 2

Inhibition of VEGFR2 and FGFR1 tyrosine kinase activity by indolinones and anilinophthalazines. Sutent, SU5416 and PTK787 differentially inhibited the intrinsic tyrosine kinase activity of (A) VEGFR2 and (B) FGFR1. Inhibition profiles were generated by incubating recombinant VEGFR2 with (radiolabelled) [γ^{32}P]-ATP and $MgCl_2$ including a concentration range for each inhibitor (0.8 nM to 80 μM). Inhibition was assessed by measuring relative reduction of [γ^{32}P]-ATP signal. Data are presented as ±SEM (n = 3); IC_{50} values were derived from the curves shown.

Table 2

Comparison of inhibitory effects of indolinones and anilinophthalazines on VEGFR2 and FGFR1 tyrosine kinase activity *in vitro*

Inhibitor	IC_{50} value (μM) VEGFR2	FGFR1
SU5416	8.88 ± 0.56	13.70 ± 0.93
Sutent	0.58 ± 0.05	0.63 ± 0.15
PTK787	0.32 ± 0.02	47.9 ± 2.90

This effect was completely blocked when cells were treated with SU5416 but only partially blocked by the presence of Sutent or PTK787 (Figure 4D). The flow cytometry profiles for plasma membrane VEGFR2 levels in both unstimulated cells and cells treated with both VEGF-A and PTK787 show considerable overlap, indicating that the cell surface levels of VEGFR2 were not substantially different under these conditions (Figure S3B). The flow cytometry profiles for cells labelled for cell surface VEGFR2 after treatment with VEGF-A with either SU5416 or Sutent revealed similar profiles to that for PTK787 (data not shown).

In a further experiment we showed that treatment of HUVECs with SU5416 alone over a prolonged period caused an increase in VEGFR2 protein levels within the cell, leaving VEGFR1 levels unaffected (Figure 4E). A twofold increase in VEGFR2 levels was seen after 24 h treatment with SU5416 (Figures 4E and S3C). A similar effect was observed during incubation with either Sutent or PTK787 for the same period (data not shown).

In addition we examined the subcellular localization of FGFR1 in primary endothelial cells and also any effects of indolinones and anilinophthalazines on the trafficking of this receptor (Figure S4). In permeabilized cells, FGFR1 is localized to tubular structures, which do not co-distribute with the endosomal marker EEA-1 or a key component of the microtubule cytoskeleton, α-tubulin (Figure S4A). In non-permeabilized cells, FGFR1 appears to be found in discrete puncta resembling plasma membrane microdomains (Figure S4B), although cell surface biotinylation studies suggest only a relatively small cell surface pool of FGFR1 (Figure 4C). Treatment with bFGF for up to 180 min in the presence or absence of SU5416, Sutent or PTK787 did not alter this distribution pattern (Figure S4B). Unlike VEGFR2, treatment of primary endothelial cells with SU5416 alone for up to 24 h did not alter total expression of FGFR1 (Figure S4C). An identical result was obtained during treatment with either Sutent or PTK787 (data not shown).

Indolinones and anilinophthalazines do not selectively inhibit endothelial cell function and inhibit both VEGF-A- and bFGF-mediated endothelial cell migration and wound closure

The VEGF-VEGFR axis is important for endothelial cell migration as an early event during angiogenesis (Bruns *et al.*, 2010). A simple *in vitro* model that recapitulates early events during angiogenesis is a scratch wound assay using confluent endothelial cell monolayers. A denuded region was created in a monolayer and the migration of cells into the wounded region was monitored over 24 h in the presence of different inhibitors. In the presence of exogenous VEGF-A alone, average endothelial wound closure was ~39% (Figure 5A). Sutent, PTK787 and SU5416 all showed dose-dependent inhibition of endothelial wound closure in the presence of VEGF-A (Figure 5A) with a similar profile to that observed in signalling experiments. SU5416 was the least potent inhibitor of VEGF-A-stimulated wound closure and had no effect at 10 nM (Figure 5A). SU5416, Sutent and PTK787 exhibited differential inhibitory effects in the presence of full growth

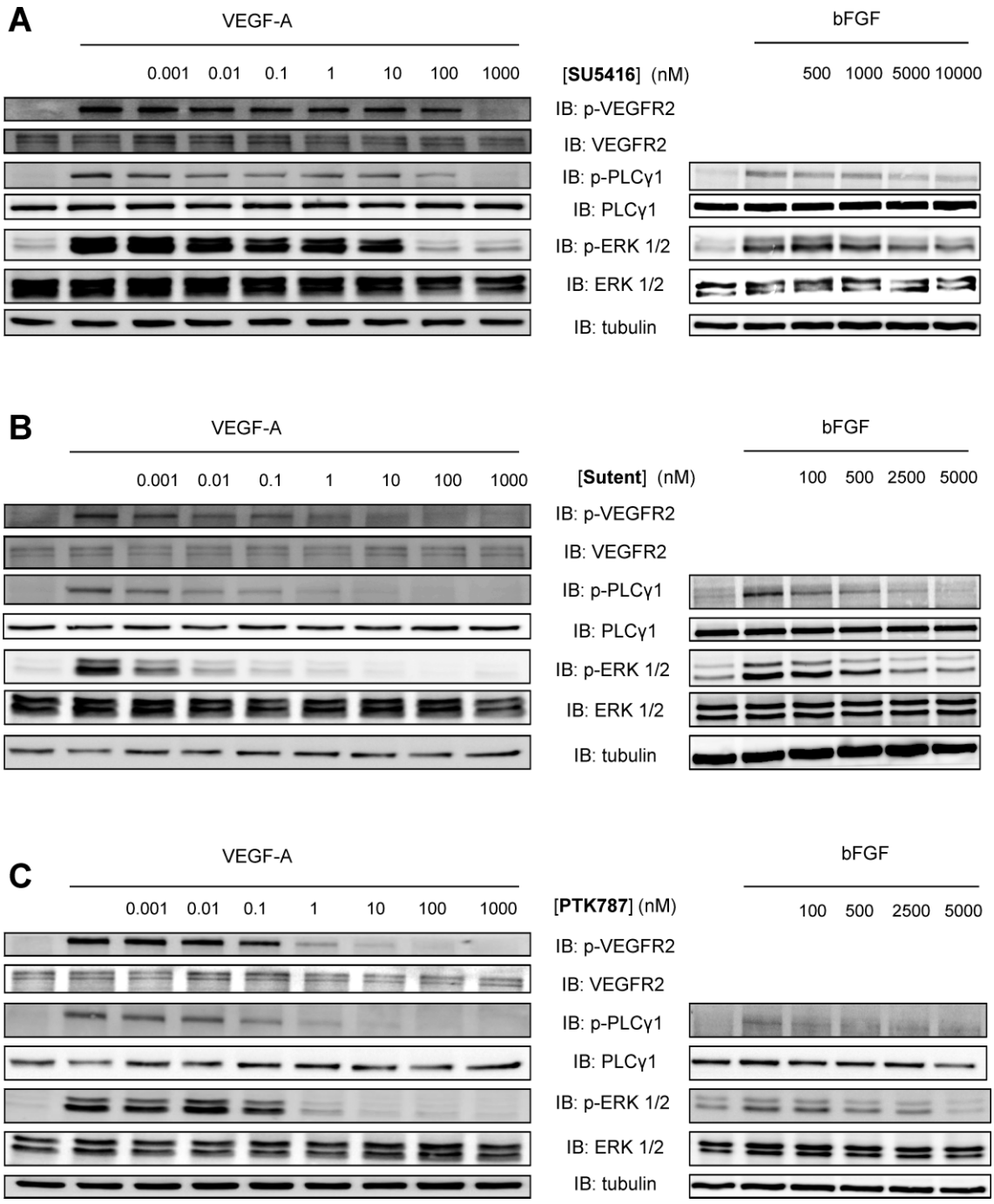

Figure 3

Dose-dependent inhibition of intracellular signalling in response to VEGF-A or bFGF in endothelial cells. (A) SU5416, (B) Sutent and (C) PTK787 each dose-dependently inhibited VEGF-A and bFGF-regulated intracellular signalling in primary endothelial cells. Cells were treated for 7.5 min with VEGF-A or bFGF (25 ng·mL^{-1}) and processed for immunoblotting using anti-phospho-PLCγ1 (Y783), anti-PLCγ1, anti-phospho-ERK1/2 (T202/Y204), anti-ERK1/2 and anti-α-tubulin antibodies. Data shown are representative of four independent experiments.

medium compared with serum-free conditions (Figures 5A, 5B and S5). In the presence of VEGF-A in serum-free medium, all three inhibitors abolished endothelial wound closure by ~70% at a concentration of 1 μM (Figure 5A). In contrast, when supplemented with full growth medium, PTK787 or SU5416 caused only ~40% inhibition of endothelial wound closure whereas Sutent displayed higher inhibition of endothelial wound closure, by ~60% (Figure 5B).

To test whether the above effects are due to inhibition of multiple receptor tyrosine kinase pathways, we examined inhibition of wound closure in different cell types. pHFF and HeLa cells exhibited 72% and 23% wound closure, respec-

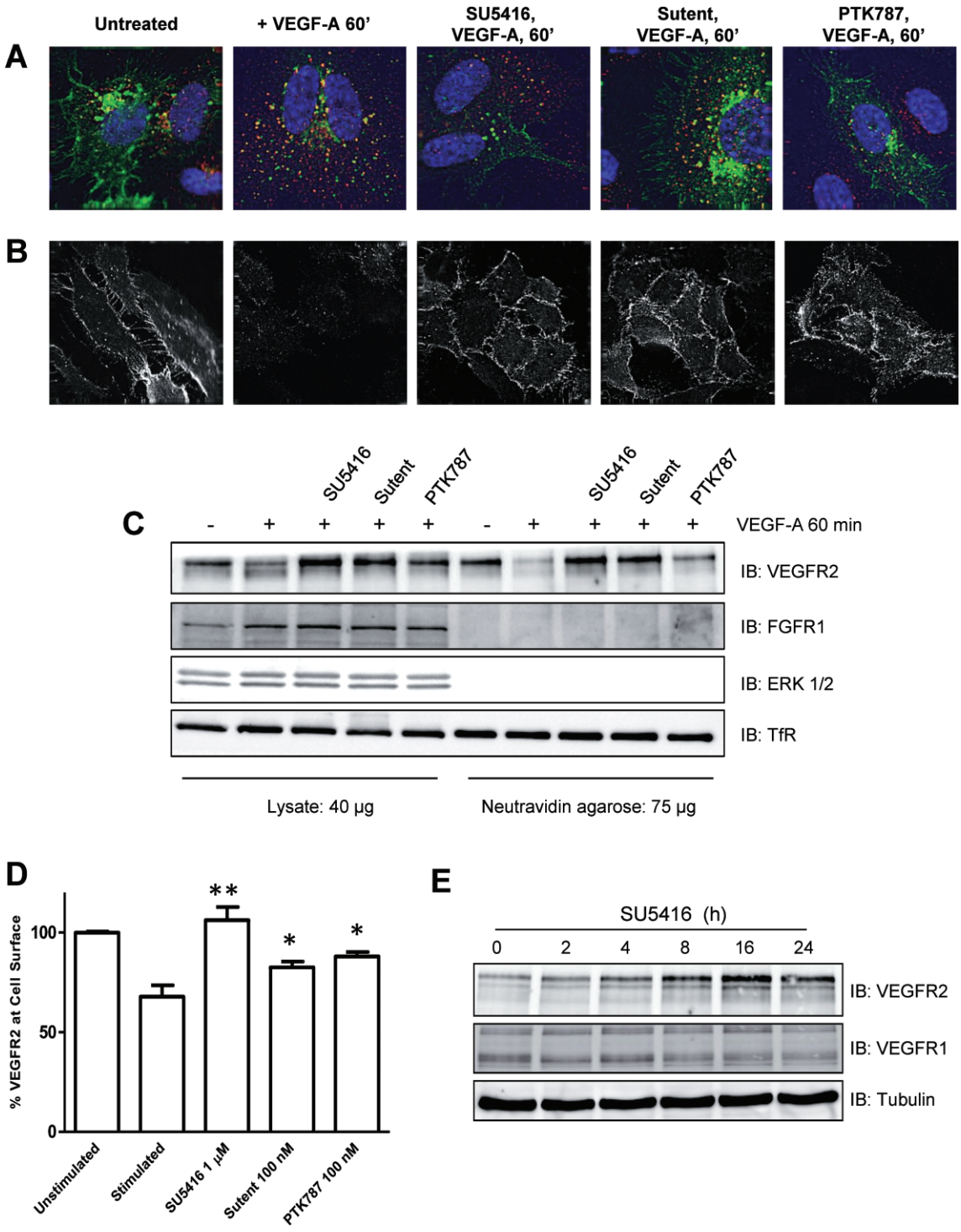

Figure 4

Indolinones and anilinophthalazines inhibit turnover, degradation and ligand-stimulated internalization of VEGFR2 in endothelial cells. (A–D) Primary endothelial cells were stimulated with VEGF-A for 60 min in the presence or absence of inhibitors. (A) Cells were fixed, permeabilized and processed for immunofluorescence microscopy using antibodies to VEGFR2 extracellular domain (green) and early endosomal antigen EEA-1 (red), followed by fluorescent labelled secondary antibodies. Nuclei were stained with DNA-binding dye, DAPI (blue). (B) Cells were not permeabilized in order to visualize only cell surface VEGFR2. (C) The cell surface was labelled with biotin and biotinylated protein complexes were precipitated on a neutravidin agarose matrix and processed for immunoblotting. (D) Cells were stained with anti-VEGFR2 and labelled secondary antibodies followed by flow cytometry analysis. (E) Cells were treated with SU5416 in full growth medium for up to 24 h. Whole cell lystes were immunoblotted with anti-VEGFR1, anti-VEGFR2 and anti-tubulin. Data are presented as normalized to control ±SEM ($n \geq 3$). Significant inhibition of VEGFR2 internalization denoted by $^{*}P < 0.05$ or $^{**}P < 0.01$ using ANOVA.

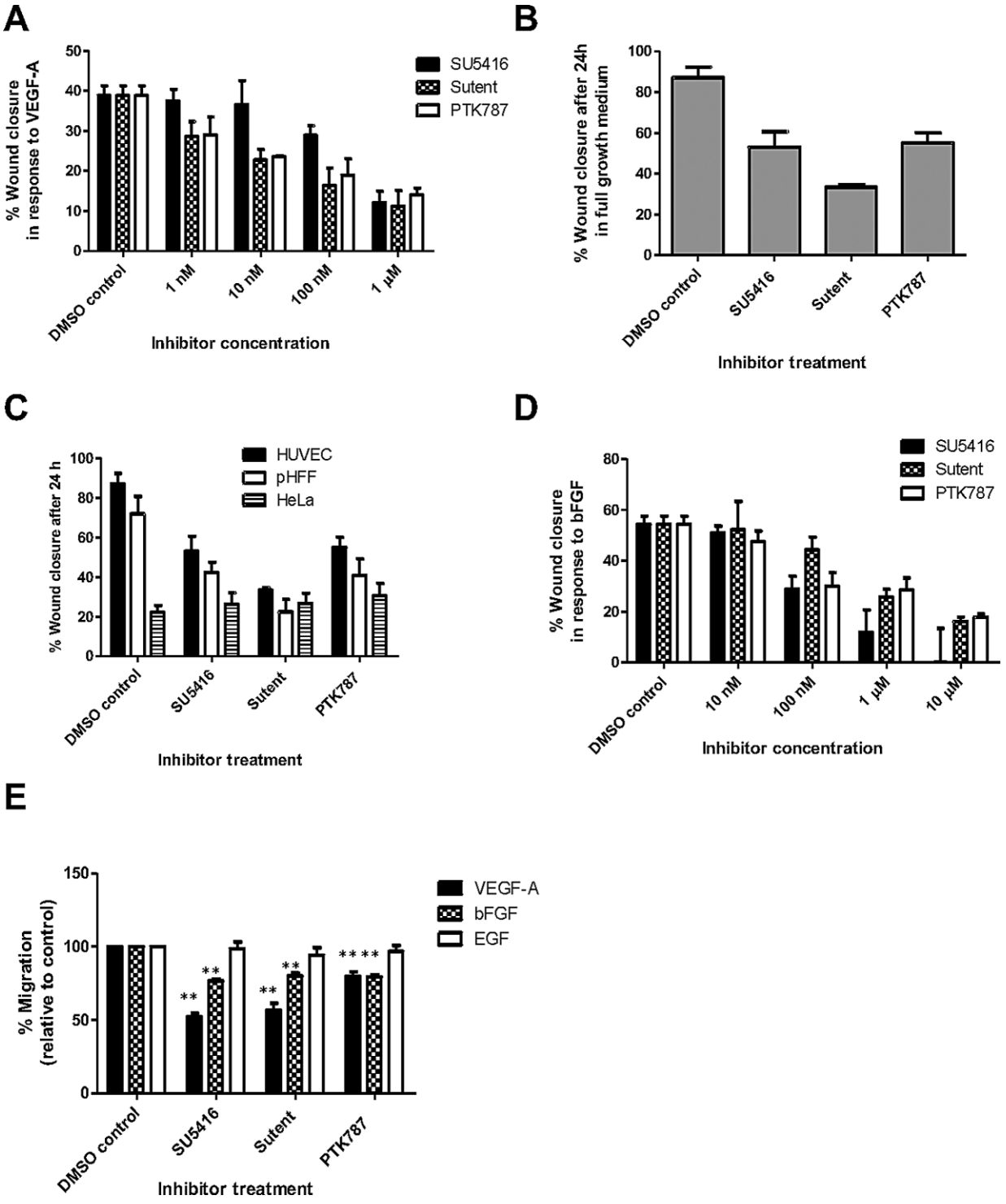

Figure 5

Selectivity of inhibition of VEGF-A-mediated endothelial cell migration and wound healing. (A) Scratch-wounded cell monolayers were stimulated with VEGF-A (25 ng·mL^{-1}) in serum-free conditions in the presence of 1 nM, 10 nM, 100 nM or 1 μM of each inhibitor. (B) Scratch-wounded cell monolayers were incubated in full growth medium in the presence of SU5416, Sutent or PTK787. (C) Ability of indolinones and anilinophthalazines to inhibit scratch wound closure in HUVEC, HeLa and pHFF cells in full growth medium [endothelial cell growth medium or Dulbecco's modified Eagle medium (DMEM)]. (D) Wounded endothelial monolayers were stimulated with bFGF (25 ng·mL^{-1}) in the presence of 10 nM, 100 nM, 1 μM or 10 μM inhibitor. All wounds were photographed before and after 24 h treatment. (E) Quantification of endothelial cell migration towards a growth factor gradient (either VEGF-A, basic FGF or EGF) in the presence of inhibitors. The inhibition of cell migration was evaluated using Student's *t*-test. Wound widths were measured using Image J software and % wound closure was calculated by [(size before – size after)/size before] × 100. Data are presented as ±SEM ($n \geq 3$). Significance denoted by $^{**}P < 0.01$.

tively, in the presence of DMSO in full tissue culture medium (Figure 5C). Both PTK787 and SU5416 inhibited wound closure by ~40% in pHFF cells, whereas Sutent inhibited wound closure by ~70% (Figure 5C). In contrast, all three compounds failed to significantly inhibit wound closure in HeLa cells (Figure 5C). This indicates that these compounds do not display selectivity towards endothelial cell function but do not target epithelial cells. What causes these observed differences? One possibility is the cellular response to FGFs such as bFGF in different cells and tissues. In the presence of exogenous bFGF alone, endothelial wound closure was ~55% (Figure 5D). Surprisingly, SU5416 was the more potent inhibitor of bFGF-mediated HUVEC wound closure, exhibiting ~80% inhibition at 1 μM. Sutent and PTK787 elicited ~50% inhibition at the same concentration (Figure 5D). To glean further insight into the selectivity of these compounds for the different cell lines, we examined the relative expression of VEGFR2 and FGFR1 in HeLa, pHFF and HUVECs by performing immunoblotting on whole cell lysates compared with known amounts of recombinant receptors (Figure S5A, B and Table S1). Only HUVECs express VEGFR2 protein (Figure S5A). However, all three cell lines express differing amounts of FGFR1: HeLa > HUVEC > pHFF (Figure S5B). HUVECs express ~25% of VEGFR2 compared with FGFR1 (Table S1). These data suggest that inhibition of fibroblast wound closure by indolinones and anilinophthalazines is not due to inhibition of VEGF-A regulated pathways, but does not explain why these compounds inhibit fibroblast and not HeLa wound closure.

In addition, we subjected HUVECs to a growth factor gradient (either VEGF-A, bFGF or EGF) and allowed them to migrate across a pore-containing filter in the presence or absence of inhibitor. Under control conditions, VEGF-A and bFGF elicited the strongest migratory responses (154 ± 19 and 157 ± 14 cells per field, respectively) while EGF elicited a less pronounced response (116 ± 22 cells per field; Figure 5E). Both indolinones and anilinophthalazines inhibited VEGF-A-mediated migratory responses in HUVECs to differing extents, SU5416 having the greatest inhibitory effect (~50% inhibition) and PTK787 having the least inhibitory effect (~20% inhibition). All three compounds inhibited bFGF-mediated migration to the same extent (~20% inhibition) whereas they failed to significantly inhibit an EGF-mediated migratory response in HUVECs (Figure 5E).

Since indolinones and anilinophthalazines inhibit signalling through the ERK1/2 pathway in HUVECs, we also examined drug inhibition of cellular proliferation. Using both an MTS-based cell proliferation assay and a BrdU uptake ELISA, it was shown that neither drug significantly inhibited cell proliferation in the concentration range 1 nM to 1 μM ($P < 0.05$) (Figure S6B).

Indolinones and anilinophthalazines inhibit endothelial tube formation in the presence of both VEGF-A and bFGF

The ability of endothelial cells to form into three-dimensional tubular structures is critical for lumen formation during blood vessel sprouting (Olsson *et al.*, 2006). Here we use an *in vitro* co-culture model in which endothelial cells in the presence of either VEGF-A or bFGF form hollow tubes on top of a confluent fibroblast monolayer. In order to assess the effects of indolinones and anilinophthalazines on tube formation we measured both the tubule length and the number of tubule branch points. SU5416 was the weakest inhibitor of tube formation (Figure 6A). At 100 nM, SU5416 inhibited VEGF-A-stimulated tube length growth by ~31% and tube branch formation by ~64%. However, at the same concentration, SU5416 failed to significantly inhibit bFGF-mediated tubulogenesis. At a higher concentration, 1 μM, SU5416 inhibited bFGF-driven tube formation by 90% or more (Figure 6B and C). Sutent was the more potent inhibitor of tube formation and showed almost complete inhibition of VEGF-A- and bFGF-mediated events at either 100 nM or 1 μM (Figure 6). It is important to note that lack of tube formation during inhibitor treatment is not due to compound toxicity, as endothelial cells remained alive and adherent in visible 'islands' (Figure 6A, see Sutent treatment). PTK787 was a potent inhibitor of bFGF-driven tubulogenesis, but displayed only ~53% inhibition of VEGF-A-stimulated tube formation at 100 nM (Figure 6C). At a 10-fold higher concentration PTK787 abolished almost all tubulogenesis in the presence of both growth factors (Figure 6).

Discussion

Indolinones and anilinophthalazines are classes of small molecule tyrosine kinase inhibitors and are an attractive alternative to traditional chemotherapeutic agents for treatment of cancer (Roskoski, 2007). Their mechanism of inhibition of VEGFR2 kinase activity has been well characterized (Mendel *et al.*, 2000a; 2003; Wood *et al.*, 2000); however, neither inhibitor studied here is specific for VEGFR2. SU5416 also inhibits c-Kit and Flt-3 (Mendel *et al.*, 2000a). PTK787 inhibits VEGFR1, VEGFR3, platelet-derived growth factor receptor (PDGFR) beta, c-Kit and c-Fms (Lin *et al.*, 2002). Sutent is described as one of the most promiscuous tyrosine kinase inhibitors (Karaman *et al.*, 2008) and inhibits the PDGFR, c-Kit and Flt-3 kinases (Mendel *et al.*, 2003; Hasinoff & Patel, 2010). Hence, the target specificity of these inhibitors is under much discussion in the pharmaceutical industry. A number of studies suggest that indolinones and anilinophthalazines are not active against FGFRs (Fong *et al.*, 1999; Takamoto *et al.*, 2001; Arora & Scholar, 2005; Rini & Small, 2005). Here we show that these chemically and structurally distinct compounds exhibit some (in the case of Sutent, very potent) *in vitro* activity against FGFR1 and elicit differential effects on VEGF-A- and bFGF-mediated signalling and angiogenic outputs such as cell migration and tube formation.

The indolinones are predicted to make hydrogen bond contacts in the hinge region of both kinase domains; however, anilinophthalazines make contact with the 'DFG motif' of both VEGFR2 and FGFR1. Inhibitor binding here can either lock the kinase domain in an inactive or 'DFG-out' conformation, such as the bcr-abl inhibitor imatinib, or in a near-active 'DFG-in' state to prevent ATP binding (Zhou *et al.*, 2010). Currently, there are no published X-ray co-crystal structures of PTK787 bound to either of the receptor tyrosine kinase domains. The indolinone SU5416 is a weaker inhibitor of VEGFR2 kinase activity compared with Sutent and PTK787, but exhibits a much steeper inhibitory profile of VEGF-A mediated signalling. In contrast, PTK787 is the weakest

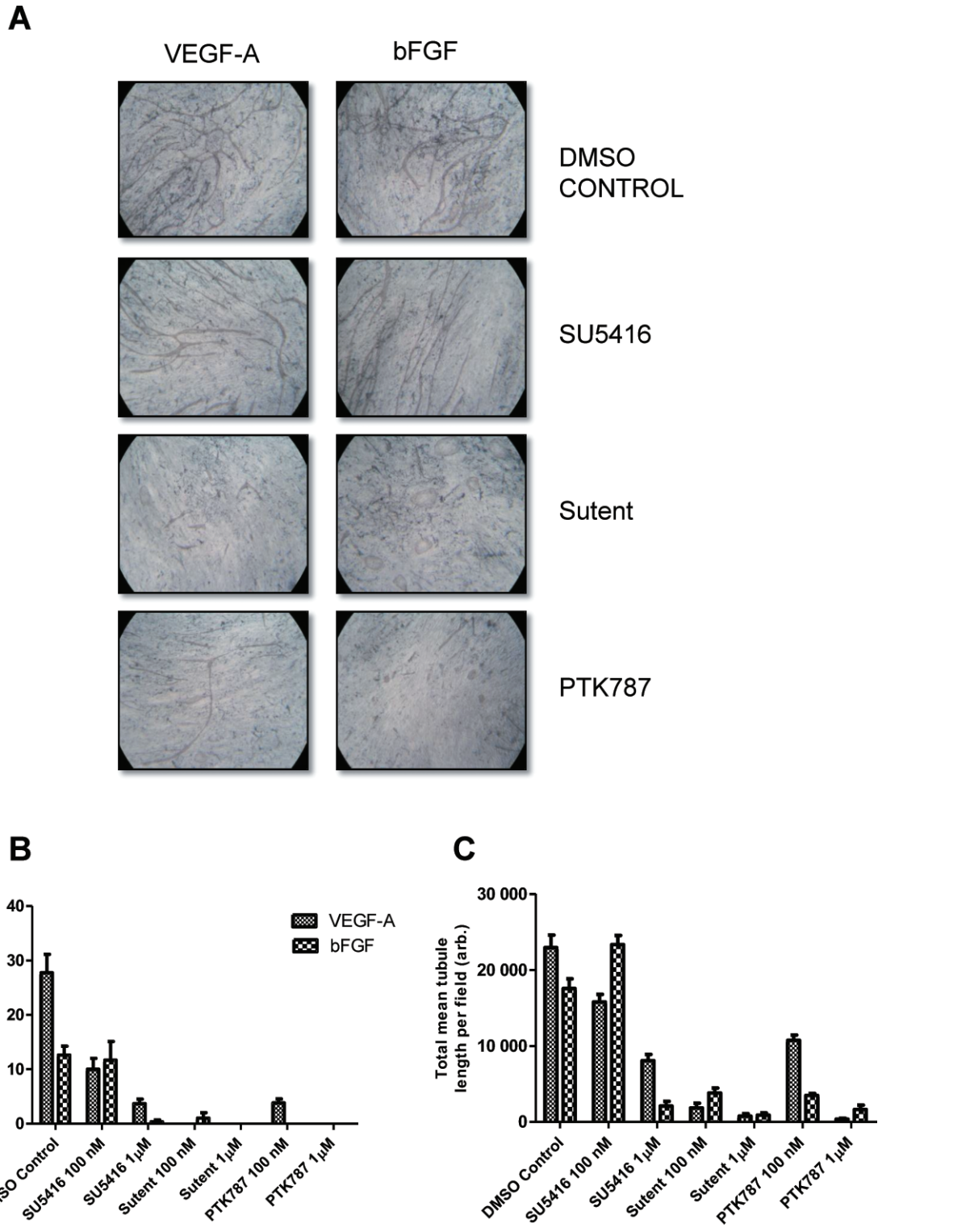

Figure 6

Indolinones and anilinophthalazines inhibit endothelial tube formation in response to VEGF-A and bFGF. (A) Endothelial tubulogenesis stimulated by the presence of VEGF-A or bFGF in an endothelial-fibroblast co-culture model was evaluated for the effects of SU5416, Sutent or PTK787 over a 7 day period. (B) Quantification of endothelial tube branch formation, and (C) quantification of endothelial tube length formation by indolinones or anilinophthalazines. Quantification performed using Image J software. Data are presented as ±SEM ($n \geq 6$).

inhibitor of the FGFR1 kinase. Sutent exhibits potent inhibition of both receptors. Mostly, these properties are reflected in the ability of the compounds to inhibit intracellular signalling stimulated by VEGF-A and bFGF.

Our findings suggest that these inhibitors are more potent in a cell-based system than in a cell-free system, a phenomenon also observed in other studies (Tille *et al.*, 2001). One hypothesis is that isolated protein under non-physiological ATP concentrations in an *in vitro* assay produces different results than in cells. It has also been reported that these compounds have long-lasting effects owing to their intracellular accumulation (Mendel *et al.*, 2000b). We thus highlight the importance of using cell-based methods to better represent an *in vivo* setting when elucidating the mechanism of action of pharmacological agents. It is suggested that bFGF-induced angiogenesis is partially the result of activating an autocrine loop involving increased synthesis of VEGF-A, VEGF-C and VEGFR2 and that the inhibitors block the response of newly synthesized ligands (Tille *et al.*, 2001). For SU5416 and PTK787, this may in part explain the discrepancy between weaker FGFR kinase inhibition but potent inhibition of bFGF-mediated responses.

Although we could not demonstrate that bFGF induces tyrosine phosphorylation of FGFR1 in endothelial cells, we cannot rule out this possibility as we and others have shown extremely low plasma membrane FGFR1 levels in primary endothelial cells, suggesting that this could still occur but is outside the limits of current methods of detection (Garfinkel *et al.*, 1996). Thus, the classical and most acceptable approach towards studying FGFR-related activation is to examine phosphorylation of key FGFR1-associated adaptor substrates (e.g. cortactin, Src and PLCγ) and downstream signalling proteins (e.g. ERK1/2) (Garfinkel *et al.*, 1996). It has been shown that FGFR1 is essential for bFGF-mediated signalling in bovine endothelial cells (Tanghetti *et al.*, 2002) and post-capillary venous endothelial cells (Finetti *et al.*, 2008). An alternative possibility is that bFGF binds to and activates FGFR2, FGFR3 or FGFR4 in HUVECs. However, it is widely accepted that FGFR1 is the most highly expressed family member in endothelial cells (Antoine *et al.*, 2005; Nourse *et al.* 2007; Murakami *et al.*, 2008) and there is uncertainty as to whether the other FGFR genes are expressed at all (Antoine *et al.*, 2005; Nourse *et al.* 2007). Finally, FGFs can signal non-canonically through cell surface syndecan-4, independent of FGFRs, although signalling to the MAPK pathway has not been demonstrated by this interaction (Murakami *et al.*, 2008).

In addition to inhibiting receptor activation and signalling, we showed that indolinones and anilinophthalazines alter VEGFR2 trafficking. Treatment with these compounds increased VEGFR2 protein levels in endothelial cells. They also prevented ligand-stimulated VEGFR2 internalization, leading to plasma membrane VEGFR2 accumulation. These findings suggest that indolinones and anilinophthalazines retard VEGFR2 degradation and turnover by interfering with both ligand-dependent and -independent trafficking pathways. Further work is needed to explore the significance of this inhibition: to what extent is VEGFR2 phosphorylation a prerequisite for its ubiquitination? How do alterations in VEGFR2 sub-cellular localization affect its processing and proteolysis? One possibility is that manipulation of VEGFR2 activity and localization by use of inhibitors can alter processing and downstream signalling linked to pro-angiogenic outputs (Bruns *et al.*, 2010). Importantly, FGFR1 localization and levels are not altered in response to bFGF in HUVECs, nor are they affected by indolinones and anilinophthalazines, indicating that this receptor is not the main focus of bFGF-mediated downstream responses.

In the present study, SU5416, Sutent and PTK787 dose-dependently inhibit endothelial scratch wound closure; however, we showed that only a proportion of this observation was due to inhibition of the VEGF-A-VEGFR2 axis. This is based on three lines of evidence. Firstly, all three compounds significantly inhibited wound closure in full growth medium, in which bFGF is a major supplemented growth factor. Secondly, the compounds did not selectively inhibit endothelial function but also inhibited wound closure in fibroblasts. The off-target inhibition of fibroblasts may have more serious consequences for cardiovascular function and tissue regeneration: the lack of target specificity of Sutent and PTK787 has recently been correlated with myocyte damage and cardiotoxicity (Hasinoff and Patel, 2010). In contrast, indolinones and anilinophthalazines failed to inhibit wound closure in HeLa cells, despite these cells expressing a high amount of FGFR1. These cells of epithelial origin also possess high EGF receptor copy number (Schoeberl *et al.*, 2002). Finally, to corroborate our conclusions, we showed that indolinones and anilinophthalazines inhibit endothelial cell migration and wound closure in response to both a VEGF-A and bFGF gradient, but do not affect cell migration along an EGF gradient. Neither indolinones nor anilinophthalazines inhibit endothelial cell proliferation at the concentrations used in this study. Such lack of efficacy has been noted for similar compounds (Tille *et al.*, 2001). This suggests that the inhibitory effects of the drugs on wound healing and angiogenic tubule formation are primarily due to their effects on cell migration.

The primary sequences of the VEGFR and FGFR kinase domains are highly homologous. Several dual FGFR-VEGFR tyrosine kinase inhibitors are currently under development, for example, brivanib (BMS), TKI-258 (Novartis), Vargatef (Boehringer Ingleheim) and RO438596 (Roche) (Knights and Cook, 2010). Specific targeting of the endothelial VEGF-VEGFR axis may not be sufficient to inhibit the growth of cancers, as the VEGF system exhibits considerable redundancy (Arora and Scholar, 2005). In addition, the FGF-FGFR signalling pathway can drive resistance for tumours subject to anti-VEGF therapy (Knights and Cook, 2010; Oguro *et al.*, 2010). Multi-kinase inhibition (e.g. VEGFR and FGFR) may thus be a useful property of anti-angiogenic drugs, but can also be a double-edged sword: simultaneous inhibition of a panel of tyrosine kinases may have detrimental consequences for homeostatic endothelial function (e.g. blood pressure regulation). Non-specific off-target inhibition of serine-threonine kinases may lead to collateral toxicity (Hasinoff and Patel, 2010) owing to severe side effects, as have been noted in PTK787 clinical trials (Eskens, 2004; Los *et al.*, 2007). To this end, we hypothesize that the pharmacological profile of the inhibitors reflects their performance in clinical trials, for example, SU5416 has a narrow working concentration range, is relatively ineffective at low doses and highly potent and toxic at higher doses, indicating that it is unlikely to be a good choice for clinical use. However, its properties make it

a useful laboratory tool. SU5416 has been withdrawn from clinical trials due to lack of efficacy, toxicity and difficulties in administration (Eskens, 2004; Jubb *et al*. 2006). Sutent is potent, broad-spectrum and is the only inhibitor of the three that has been approved for clinical use (Roskoski, 2007). Work is needed to further explore the specificity of these inhibitors, in particular to examine effects on VEGFR1, VEGFR3 and FGFRs. The methods used in this study and other cell-based assays, for example fibroblast co-culture assays, could provide an effective means of validating or eliminating lead compounds in the early stages of the drug development pipeline. It is proposed that *in silico* modelling studies have now exhausted all chemical scaffolds of ATP-competitive kinase inhibitors (Zhang *et al*., 2009), thus one approach is to ameliorate existing compounds, for which studies such as this would bring invaluable insight.

In summary, we revealed novel mechanisms of action of indolinones and anilinophthalazines. In particular, the anti-cancer drug Sutent displayed equally potent inhibition of VEGFR2 and FGFR1 tyrosine kinase activity *in vitro* and both VEGF-A- and bFGF-mediated responses in endothelial cells. For the first time we also showed that these drugs exert their effects by modulating receptor tyrosine kinase trafficking. The effects of these drugs on receptor tyrosine kinase activity can be translated into even more potent effects on endothelial function, cell migration and tubulogenesis. Thus, we provide a large body of evidence that indolinones and anilinophthalazines are true multi-kinase inhibitors.

Acknowledgements

This work was supported by a BBSRC-CASE PhD studentship from Pfizer Global (A. M. L) and a Wellcome Trust project grant (S. P.). We thank Leyuan Bao, Gareth Howell and Adam Odell for help and advice.

Conflict of interest

The authors state no conflict of interest.

References

Ali MA, Bhogal N, Findlay JB, Fishwick CW (2005). The first de novo-designed antagonists of the human NK(2) receptor. J Med Chem 48: 5655–5658.

Antoine M, Wirz W, Tag CG, Mavituna M, Emans N, Korff T *et al*. (2005). Expression pattern of fibroblast growth factors (FGFs), their receptors and antagonists in primary endothelial cells and vascular smooth muscle cells. Growth Factors 23: 87–95.

Arora A, Scholar EM (2005). Role of tyrosine kinase inhibitors in cancer therapy. J Pharmacol Exp Ther 315: 971–979.

Bae JH, Boggon TJ, Tome F, Mandiyan V, Lax I, Schlessinger J (2010). Asymmetric receptor contact is required for tyrosine autophosphorylation of fibroblast growth factor receptor in living cells. Proc Natl Acad Sci USA 107: 2866–2871.

Blanes MG, Oubaha M, Rautureau Y, Gratton JP (2007). Phosphorylation of tyrosine 801 of vascular endothelial growth factor receptor-2 is necessary for Akt-dependent endothelial nitric-oxide synthase activation and nitric oxide release from endothelial cells. J Biol Chem 282: 10660–10669.

Bruns AF, Herbert SP, Odell AF, Jopling HM, Hooper NM, Zachary IC *et al*. (2010). Ligand-stimulated VEGFR2 signaling is regulated by co-ordinated trafficking and proteolysis. Traffic 11: 161–174.

Carmeliet P (2003). Angiogenesis in health and disease. Nat Med 9: 653–660.

Chow LQ, Eckhardt SG (2007). Sunitinib: from rational design to clinical efficacy. J Clin Oncol 25: 884–896.

Eskens FA (2004). Angiogenesis inhibitors in clinical development; where are we now and where are we going? Br J Cancer 90: 1–7.

Ewan LC, Jopling HM, Jia H, Mittar S, Bagherzadeh A, Howell GJ *et al*. (2006). Intrinsic tyrosine kinase activity is required for vascular endothelial growth factor receptor 2 ubiquitination, sorting and degradation in endothelial cells. Traffic 7: 1270–1282.

Ferrara N, Gerber HP, Lecouter J (2003). The biology of VEGF and its receptors. Nat Med 9: 669–676.

Finetti F, Solito R, Morbidelli L, Giachetti A, Ziche M, Donnini S (2008). Prostaglandin E2 regulates angiogenesis via activation of fibroblast growth factor receptor-1. J Biol Chem 283: 2139–2146.

Fong TA, Shawver LK, Sun L, Tang C, App H, Powell TJ *et al*. (1999). SU5416 is a potent and selective inhibitor of the vascular endothelial growth factor receptor (Flk-1/KDR) that inhibits tyrosine kinase catalysis, tumor vascularization, and growth of multiple tumor types. Cancer Res 59: 99–106.

Friesner RA, Banks JL, Murphy RB, Halgren TA, Klicic JJ, Mainz DT *et al*. (2004). Glide: a new approach for rapid, accurate docking and scoring. 1. Method and assessment of docking accuracy. J Med Chem 47: 1739–1749.

Garfinkel S, Hu X, Prudovsky IA, McMahon GA, Kapnik EM, McDowell SD *et al*. (1996). FGF-1-dependent proliferative and migratory responses are impaired in senescent human umbilical vein endothelial cells and correlate with the inability to signal tyrosine phosphorylation of fibroblast growth factor receptor-1 substrates. J Cell Biol 134: 783–791.

Harris PA, Boloor A, Cheung M, Kumar R, Crosby RM, Davis-Ward RG *et al*. (2008). Discovery of 5-[[4-[(2,3-dimethyl-2H-indazol-6-yl)methylamino]-2-pyrimidinyl]amino]-2-methyl-benzenesulfonamide (Pazopanib), a novel and potent vascular endothelial growth factor receptor inhibitor. J Med Chem 51: 4632–4640.

Hasinoff BB, Patel D (2010). The lack of target specificity of small molecule anticancer kinase inhibitors is correlated with their ability to damage myocytes in vitro. Toxicol Appl Pharmacol 249: 132–139.

Holmes K, Roberts OL, Thomas AM, Cross MJ (2007). Vascular endothelial growth factor receptor-2: structure, function, intracellular signalling and therapeutic inhibition. Cell Signal 19: 2003–2012.

Howell GJ, Herbert SP, Smith JM, Mittar S, Ewan LC, Mohammed M *et al*. (2004). Endothelial cell confluence regulates Weibel-Palade body formation. Mol Membr Biol 21: 413–421.

Jain KK (2007). Cancer biomarkers: current issues and future directions. Curr Opin Mol Ther 9: 563–571.

Jubb AM, Oates AJ, Holden S, Koeppen H (2006). Predicting benefit from anti-angiogenic agents in malignancy. Nat Rev Cancer 6: 626–635.

Karaman MW, Herrgard S, Treiber DK, Gallant P, Atteridge CE, Campbell BT *et al.* (2008). A quantitative analysis of kinase inhibitor selectivity. Nat Biotechnol 26: 127–132.

Knights V, Cook SJ (2010). De-regulated FGF receptors as therapeutic targets in cancer. Pharmacol Ther 125: 105–117.

Latham AM, Molina-Paris C, Homer-Vanniasinkam S, Ponnambalam S (2010). An integrative model for vascular endothelial growth factor A as a tumour biomarker. Integr Biol (Camb) 2: 397–407.

Lin B, Podar K, Gupta D, Tai YT, Li S, Weller E *et al.* (2002). The vascular endothelial growth factor receptor tyrosine kinase inhibitor PTK787/ZK222584 inhibits growth and migration of multiple myeloma cells in the bone marrow microenvironment. Cancer Res 62: 5019–5026.

Los M, Roodhart JM, Voest EE (2007). Target practice: lessons from phase III trials with bevacizumab and vatalanib in the treatment of advanced colorectal cancer. Oncologist 12: 443–450.

Mendel DB, Laird AD, Smolich BD, Blake RA, Liang C, Hannah AL *et al.* (2000a). Development of SU5416, a selective small molecule inhibitor of VEGF receptor tyrosine kinase activity, as an anti-angiogenesis agent. Anticancer Drug Des 15: 29–41.

Mendel DB, Schreck RE, West DC, Li G, Strawn LM, Tanciongco SS *et al.* (2000b). The angiogenesis inhibitor SU5416 has long-lasting effects on vascular endothelial growth factor receptor phosphorylation and function. Clin Cancer Res 6: 4848–4858.

Mendel DB, Laird AD, Xin X, Louie SG, Christensen JG, Li G *et al.* (2003). In vivo antitumor activity of SU11248, a novel tyrosine kinase inhibitor targeting vascular endothelial growth factor and platelet-derived growth factor receptors: determination of a pharmacokinetic/pharmacodynamic relationship. Clin Cancer Res 9: 327–337.

Murakami M, Elfenbein A, Simons M (2008). Non-canonical fibroblast growth factor signalling in angiogenesis. Cardiovasc Res 78: 223–231.

Noble ME, Endicott JA, Johnson LN (2004). Protein kinase inhibitors: insights into drug design from structure. Science 303: 1800–1805.

Nourse MB, Rolle MW, Pabon LM, Murry CE (2007). Selective control of endothelial cell proliferation with a synthetic dimerizer of FGF receptor-1. Lab Invest 87: 828–835.

Oguro Y, Miyamoto N, Takagi T, Okada K, Awazu Y, Miki H *et al.* (2010). N-phenyl-N'-[4-(5H-pyrrolo[3,2-d]pyrimidin-4-yloxy)phenyl] ureas as novel inhibitors of VEGFR and FGFR kinases. Bioorg Med Chem 18: 7150–7163.

Olsson AK, Dimberg A, Kreuger J, Claesson-Welsh L (2006). VEGF receptor signalling – in control of vascular function. Nat Rev Mol Cell Biol 7: 359–371.

Rini BI, Small EJ (2005). Biology and clinical development of vascular endothelial growth factor-targeted therapy in renal cell carcinoma. J Clin Oncol 23: 1028–1043.

Roskoski R Jr (2007). Sunitinib: a VEGF and PDGF receptor protein kinase and angiogenesis inhibitor. Biochem Biophys Res Commun 356: 323–328.

Schoeberl B, Eichler-Jonsson C, Gilles ED, Muller G (2002). Computational modeling of the dynamics of the MAP kinase cascade activated by surface and internalized EGF receptors. Nat Biotechnol 20: 370–375.

Shalaby F, Rossant J, Yamaguchi TP, Gertsenstein M, Wu XF, Breitman ML *et al.* (1995). Failure of blood-island formation and vasculogenesis in Flk-1-deficient mice. Nature 376: 62–66.

Takahashi T, Shibuya M (1997). The 230 kDa mature form of KDR/Flk-1 (VEGF receptor-2) activates the PLC-gamma pathway and partially induces mitotic signals in NIH3T3 fibroblasts. Oncogene 14: 2079–2089.

Takamoto T, Sasaki M, Kuno T, Tamaki N (2001). Flk-1 specific kinase inhibitor (SU5416) inhibited the growth of GS-9L glioma in rat brain and prolonged the survival. Kobe J Med Sci 47: 181–191.

Tanghetti E, Ria R, Dell'Era P, Urbinati C, Rusnati M, Ennas MG *et al.* (2002). Biological activity of substrate-bound basic fibroblast growth factor (FGF2): recruitment of FGF receptor-1 in endothelial cell adhesion contacts. Oncogene 21: 3889–3897.

Tasker AS, Patel VF (2008). Discovery of motesanib. DOI:10.2210/pdb3efl/pdb.

Tille JC, Wood J, Mandriota SJ, Schnell C, Ferrari S, Mestan J *et al.* (2001). Vascular endothelial growth factor (VEGF) receptor-2 antagonists inhibit. J Pharmacol Exp Ther 299: 1073–1085.

Turner N, Grose R (2010). Fibroblast growth factor signalling: from development to cancer. Nat Rev Cancer 10: 116–129.

Wood JM, Bold G, Buchdunger E, Cozens R, Ferrari S, Frei J *et al.* (2000). PTK787/ZK 222584, a novel and potent inhibitor of vascular endothelial growth factor receptor tyrosine kinases, impairs vascular endothelial growth factor-induced responses and tumor growth after oral administration. Cancer Res 60: 2178–2189.

Zhang J, Yang PL, Gray NS (2009). Targeting cancer with small molecule kinase inhibitors. Nat Rev Cancer 9: 28–39.

Zhou T, Commodore L, Huang WS, Wang Y, Sawyer TK, Shakespeare WC *et al.* (2010). Structural analysis of DFG-in and DFG-out dual Src-Abl inhibitors sharing a common vinyl purine template. Chem Biol Drug Des 75: 18–28.

Supporting information

Additional Supporting Information may be found in the online version of this article:

Figure S1 Lack of evidence that bFGF phosphorylates FGFR1 in endothelial cells. Primary endothelial cells were stimulated with bFGF (50 ng·mL^{-1}) for 7.5 min. Cells were lysed in radioimmunoprecipitation assay buffer containing ethylenediaminetetraacetic acid buffer and tyrosine phosphorylated proteins immunoprecipitated on a Protein G Sepharose matrix. Precipitated proteins were eluted in SDS-PAGE sample buffer and samples processed for immunoblotting.

Figure S2 Quantification of immunoblots in Figure 3. (A) SU5416 (B) Sutent and (C) PTK787 each dose-dependently inhibit VEGF-A- and bFGF-mediated downstream signalling in HUVECs analysed through immunoblotting with anti-phospho-PLCγ1 (Y783), anti-PLCγ1, anti-phospho-ERK1/2 (T202/Y204), ERK1/2 and anti-α-tubulin as a loading control. Data presented normalized to stimulated control ± SEM ($n \geq 3$).

Figure S3 Indolinones and anilinophthalazines inhibit turnover, degradation and ligand-stimulated internalization of VEGFR2 in endothelial cells. (A) VEGFR2 is localized to the Golgi apparatus, early endosomes and the cell surface in

quiescent endothelial cells. Endothelial cells were fixed, permeabilized and stained for VEGFR2, the early endosomal marker EEA-1 and the Golgi marker TGN46. Other cells were left non-permeabilized, labelled with the lectin AF488-Concanavalin A on ice to highlight the cell surface and co-stained with anti-VEGFR2. (B) Flow cytometry distribution profile of PTK787-treated cells from Figure 4D. (C) Quantification of VEGFR2 levels in SU5416-treated cells in Figure 4E. Significant difference denoted by $^{**}P < 0.01$ using ANOVA.

Figure S4 Subcellular localization and expression of FGFR1 in primary endothelial cells. (A) FGFR1 localizes to tubular structures within the cell which do not co-distribute with α-tubulin or EEA-1. Cells were fixed, permeabilized and stained for FGFR1, the microtubule marker α-tubulin and the early endosomal marker EEA-1. (B) Cells were stimulated with 25 ng·mL^{-1} bFGF for 60 min in the presence or absence of 5 μM SU5416, 2.5 μM Sutent or 10 μM PTK787. Cells were not permeabilized in order to visualize only cell surface FGFR1. White arrows denote discrete FGFR1 microdomains. (C) Cells were treated with 5 μM SU5416 in full growth medium for up to 24 h and processed for immunoblotting.

Figure S5 Inhibition of endothelial scratch wound closure by indolinones and anilinophthalazines. (A) Representative scratch wounds depicting drug inhibition in full medium or serum-free medium supplemented with VEGF-A and bFGF. Quantification of these images is found in Figure 5A, B and D. (B) Expression levels of VEGFR2 and (C) Expression levels FGFR1 in HeLa, pHFF and HUVEC cells. 25 μg cell lysate from a range of passages was subjected to immunoblotting alongside a titration curve of recombinant VEGFR2 or FGFR1 proteins from 1 to 10 ng. See Table S1 for further analysis.

Figure S6 Effects of indolinones and anilinophthalazines on HUVEC proliferation. A BrdU incorporation ELISA was performed on HUVECs treated with a range of concentrations of SU5416, Sutent and PTK787 in either (A) full growth medium (B) serum-free medium supplemented with 25 ng·mL^{-1} VEGF-A or (C) serum-free medium supplemented with 25 ng·mL^{-1} bFGF. BrdU incorporation was assessed by measuring absorbance at 450 nm. (D) An MTS cell viability assay was performed on HUVECs exposed to a range of inhibitor concentrations. Amount of MTS formazan product was measures using absorbance at 490 nm. Statistical differences analysed by one-way ANOVA.

Table S1 Comparison of relative expression of VEGFR2 and FGFR1 in HeLa, pHFF and HUVEC cells

Please note: Wiley-Blackwell are not responsible for the content or functionality of any supporting materials supplied by the authors. Any queries (other than missing material) should be directed to the corresponding author for the article.